Research Report

96-24

A Novel Two Phase Doubly Salient Permanent Magnet Motor

X. Luo, D. Qin, T.A. Lipo

Wisconsin Power Electronics Research Center
University of Wisconsin-Madison
Madison WI 53706-1691

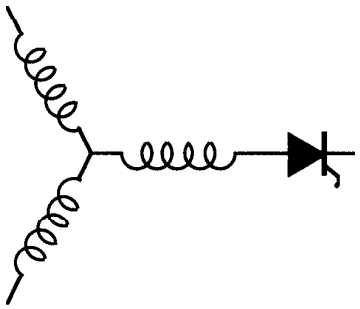

Wisconsin
Electric
Machines &
Power
Electronics
Consortium

University of Wisconsin-Madison
College of Engineering
Wisconsin Power Electronics Research Center
2559D Engineering Hall
1415 Engineering Drive
Madison WI 53706-1691

A NOVEL TWO PHASE DOUBLY SALIENT PERMANENT MAGNET MOTOR

Xiaogang Luo *Student Member, IEEE* Dinyu Qin Thomas A. Lipo *Fellow, IEEE*
Department of Electrical and Computer Engineering
University of Wisconsin-Madison
1415 Engineering Drive, Madison, WI 53705-1691, USA

Abstract— **In this paper, a dual stator, doubly salient permanent magnet motor is presented. It is shown that the machine has good power density and efficiency, and that the structure is simple and robust. By shifting one set of stator 90 electrical degrees with respect to a second set, a two phase stator winding is formed. This configuration adds the PM torque produced by each segment but cancels the reluctance torque since the reluctance torques produced by the two phase windings are out of phase. The principle of operation, finite element analysis and simulation of this new machine are investigated in the paper. Comparison is made between this new machine and the conventional VRM machine.**

I. INTRODUCTION

The concept of doubly salient permanent magnet (DSPM) machine is not new. In 1955 Rauch and Johnson presented perhaps the first doubly salient PM machine design [1]. This machine functions on the principle of the so-called flux-switching. Due to the PM materials available then, Alnico was used in the design. Thus the size of that alternator was quite large due to the low magnetic energy product of the PM material. Its simple stator and rotor punchings, however, are desirable for realizing a rugged motor structure.

As new high magnetic energy product PM materials have become available on the market, interest in the doubly salient PM machines has been renewed. The structure of doubly salient machines was further studied and two versions of three phase doubly salient PM motors were proposed and implemented by Y. Liao *et al.*[2],[3]. To obtain high air gap flux density, a football shaped stator was built to gain high flux concentration ratio to compensate for the high flux leakage associated with this particular structure resulting from locating the PM on the stator. The aspect of field weakening ability of the above motor was further explored[4].

Another version of a DSPM, which is an inside out transformation of the previous machine, was proposed[5]. This machine has 4 stator poles and 6 rotor poles. This type has high power density due to the full 180° current conduction, but has no starting torque at certain rotor positions so that it is only suitable for use as a generator.

The above mentioned DSPM designs focus attention on obtaining high power density and efficiency. The prospect of field weakening of DSPM machines has been studied by Y. Li *et al.* and a doubly salient PM generator and motor capable of field weakening(FWDSPM) were proposed[6],[7]. These machines offer improved performance, lower cost, field control capability and robust structure for applications requiring a wide field weakening operation range. The key feature of the FWDSPM is the thin magnet layer which has a low reluctance to the main flux path such that the air gap flux can be adjusted with much smaller MMF than the case with normal PM machines. Another advantage of this motor is that the field winding can strengthen the air gap flux when high flux density is in need, such as during motor starting. Since ferrite PMs are used in the design, the cost is relatively low. While not specifically addressed herein, the approach of this paper can be extended to topology of the field weakened designs of [7].

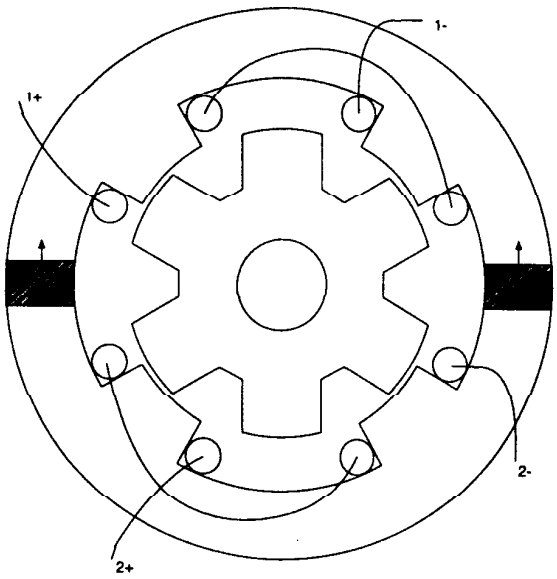

Fig. 1. Structure of a 4/6 Pole DSPM Machine

II. PRINCIPLE OF OPERATION

The structure of a 4 stator pole, 6 rotor pole(4/6 pole) single phase DSPM machine is shown in Fig. 1. For a clear understanding of the operating principle, the following assumptions are made:

1. The iron has infinite permeability,
2. The air gap flux is evenly distributed under the overlapped pole pair,
3. The fringing effect is neglected.

Having above assumptions, the flux linkage of a stator pole winding has the following features:

- When a rotor pole begins overlapping with the pole until the pole pair fully aligns, the flux linkage increases linearly,
- When the rotor pole leaves the fully aligned position until there is no overlapping between the poles, the flux linkage decreases linearly,

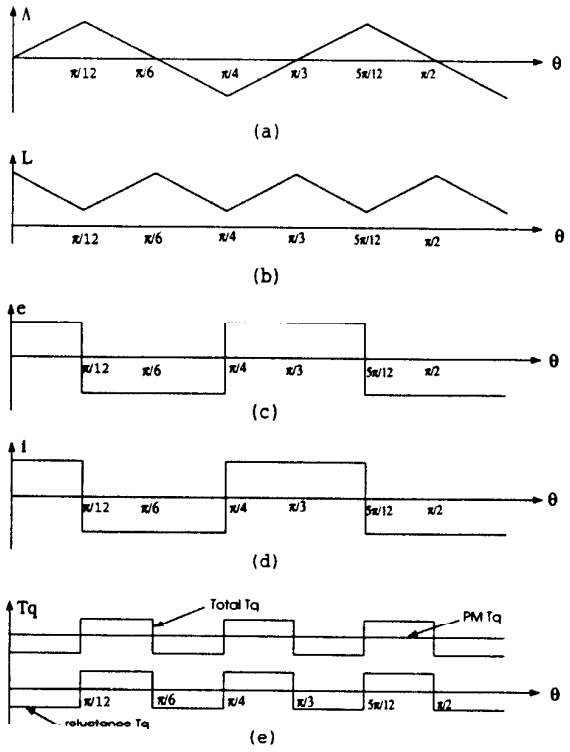

Fig. 2. Flux Linkage, Inductance, Back EMF, Current and Torque of DSPM Machine

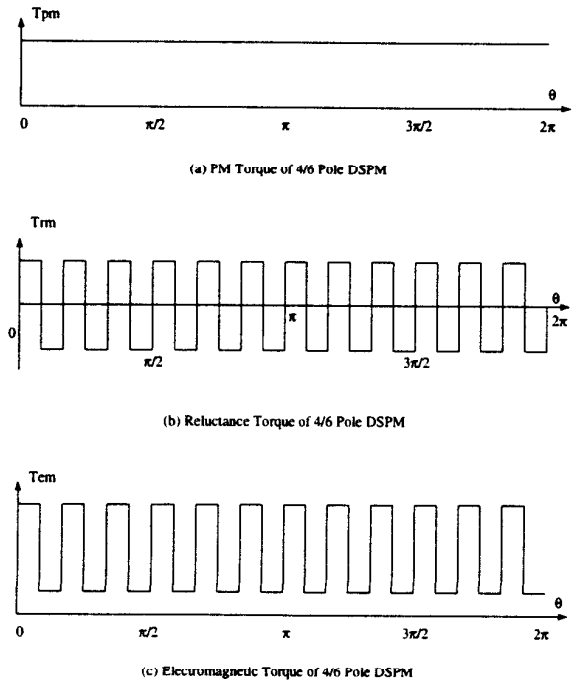

Fig. 3. Estimated Torque vs. Rotor Position Curve of 4/6 Pole DSPM Machine

As shown in Fig. 1, a stator pole always overlaps with a rotor pole at all but one rotor position. From a rotor pole starting to overlap with the stator pole to full alignment of the pole pair, the flux linkage of the pole winding due to magnets is

$$\Lambda_{pm} = \frac{D_{is}}{2} L_{eff} N_p B_g \theta \tag{1}$$

where D_{is} is the stator inner diameter, L_{eff} is the effective stack length, N_p is the number of turns per pole, B_g is the air gap flux density within the overlapped region of stator and rotor poles. θ is the overlapped angle.

The induced back emf due to PM produced flux change in the pole winding is obtained from the derivative of Λ_{pm} over time, i.e.,

$$e_p = \frac{D_{is}}{2} L_{eff} N_p B_g \omega \tag{2}$$

where ω is the rotor angular speed.

As the rotor pole leaves the aligned position, Λ_{pm} decreases linearly with respect to the variation of θ, and e_p will have a negative sign but the same magnitude. Hence, the flux linkage vs. rotor position curve and the back emf of a pole winding vs. rotor position curve takes the form shown in Fig. 2 (a) and (c).

Having obtained the back emf waveform shown in Fig. 2 (c), it is obvious that to obtain maximum power the desired current wave form should have the same form as that of the back emf as shown in Fig. 2 (d).

Observing the geometry of the machine, it be observed that the pole winding inductance varies as the rotor moves. At half alignment, the inductance reaches its maximum value. At the fully aligned position, and during the non-overlapping interval, it has a very small value. The inductance vs. rotor position curve shown in Fig. 2 (b) is a linear approximation of the inductance variation vs. rotor position.

Since there is current injected in the winding, the flux is composed of two parts: PM produced flux and current induced flux

$$\Lambda_p = \Lambda_{pm} + L_p i \tag{3}$$

The back emf is now

$$e_p = \frac{d\Lambda_p}{dt} = L_p \frac{di}{dt} + i\frac{dL_p}{dt} + \frac{d\Lambda_{pm}}{dt} \tag{4}$$

The power absorbed or generated by a pole is then

$$\begin{aligned} p_e &= e_p i = i\frac{d\Lambda_p}{dt} = iL_p\frac{di}{dt} + i^2\frac{dL_p}{dt} + i\frac{d\Lambda_{pm}}{dt} \\ &= \frac{d}{dt}[\frac{1}{2}L_p i^2] + [\frac{1}{2}i^2\frac{dL_p}{d\theta}\omega] + i\frac{d\Lambda_{pm}}{d\theta}\omega \end{aligned} \tag{5}$$

The first term represents the change of stored magnetic field energy, the second term is the power related to reluctance variation and the third term is the the power due to interaction of the PM flux and current.

The torque produced by one pole is

$$T_p = \frac{1}{2}i^2\frac{dL_p}{d\theta} + i\frac{d\Lambda_{pm}}{d\theta} = T_{prm} + T_{ppm} \tag{6}$$

where $\frac{1}{2}i^2\frac{dL_p}{d\theta}$ is the reluctance torque and $i\frac{d\Lambda_{pm}}{d\theta}$ is the PM torque. Fig. 3 shows the estimated torque waveforms. Observing Fig. 3 reveals that the reluctance torque has zero average value so that only the PM torque takes part in the energy conversion and can be used for estimating the torque capability of DSPM machine.

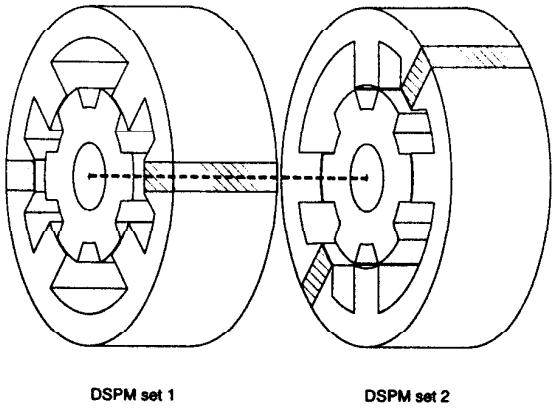

Fig. 4. Structure of 4/6 Pole Dual Stator DSPM Motor

If the desired current waveform is available, the PM power is constant when the pole is active, then at any moment the useful PM torque is produced by all 4 poles and therefore is

$$T_{pm} = 4i_{pk}\frac{d\Lambda_{pm}}{d\theta} = 4i_{pk}\frac{D_{is}}{2}L_{eff}N_pB_g \tag{7}$$

As the current takes the form of Fig. 2 (d), the peak current i_{pk} is

$$i_{pk} = \frac{(\pi D_{is}A_s)}{4\cdot(2N_p)} \tag{8}$$

where A_s is the rms surface current density. The PM torque then is

$$T_{pm} = \frac{\pi}{4}{D_{is}}^2 L_{eff}B_gA_s \tag{9}$$

It can be noted that the reluctance torque is pulsating in this machine and does not contribute to the energy conversion. Since it is proportional to the square of current, while the PM torque is in direct proportion to the current, at a certain high current level, the magnitude of reluctance torque will exceed that of the PM torque. At the fully aligned rotor position, there is neither PM torque nor reluctance torque. From above discussion, it is determined that the 4/6 pole DSPM machine has higher torque capability, symmetric current and inductance, but cannot start at certain positions, which leads to its suitability primarily for working as generator [5].

Consider, however, if two single phase DSPM machines are joined by installing two rotors on the same shaft and two stators in one machine frame. The stator or rotor of one machine can be shifted with respect to the other by 45 degrees, as shown in Fig. 4. Electrically one can then realize a two phase DSPM motor. In this case when one machine is at its fully aligned position, the other machine is exactly at its half aligned position. Electrically the two sets of windings are 90° out of phase. Since the frequency of reluctance torque pulsating is double that of current, the reluctance torques produced by the two sets are 180° out of phase, so that they essentially cancel each other completely. Fig. 5 shows this situation.

Since each member of the set has the same structure as that of a single phase DSPM generator, the variation of flux linkage, inductance and back emf are the same as those of the single phase case. The torque capability is similar, however, now the L_{eff} is the sum of two stator stack lengths.

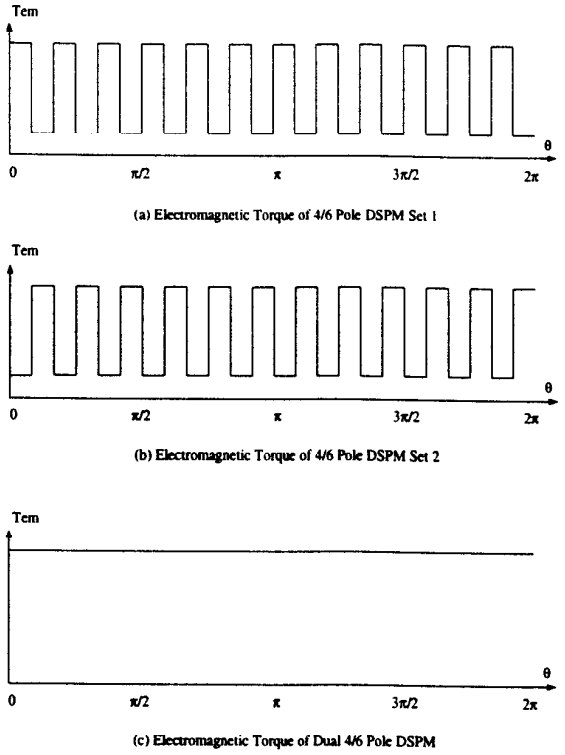

Fig. 5. Electromagnetic Torque of Dual Stator DSPM

Since this new structure has two stator and rotor stacks, there is no electromagnetic coupling between these two sets. Therefore, a space must be provided for an end winding region between the two sets of stators. The axial length of the effective stack length is the same as that of the same rating/speed single DSPM generator, but the real length including the space for end winding is larger than that of the DSPM generator. Of course, extra copper is needed for the extra end winding. Overall, considering the gains earned, such as higher torque capability compared to a 6 pole stator/4 pole rotor DSPM structure [5], smooth torque and good starting torque, the cost of a somewhat larger size and the additional copper can be justified.

III. Finite Element Analysis

Finite element analysis can be used for establishing the static, nonlinear modeling and performance estimation needed to evaluate the dual stator DSPM ($(DS)^2PM$) motor. The magnetic saturation of the iron, fringing effect and armature reaction are all accounted for by the FEM analysis. After a field solution was obtained, the flux linkage and winding inductances were further calculated. The package used was the ANSOFT's Maxwell 2D simulator, a general purpose field analysis package.

Fig. 6 shows the flux distribution of the $(DS)^2PM$ motor under a no load condition (no winding current) when the rotor poles and stator poles are half aligned. Since only the PM excitation is present, two pairs of poles receive half of the total flux. The flux density in the air gap within the overlapped area is about 1.3 tesla while the flux density in the PM is about 0.9 tesla. The flux distribution of the $(DS)^2PM$ motor under no load, with two pairs of stator and rotor poles fully

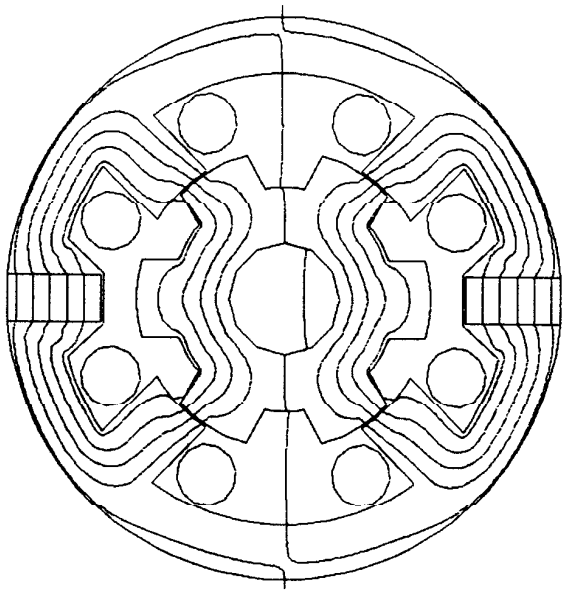

Fig. 6. Flux Distribution of $(DS)^2$PM Motor – Half Aligned Position without Current

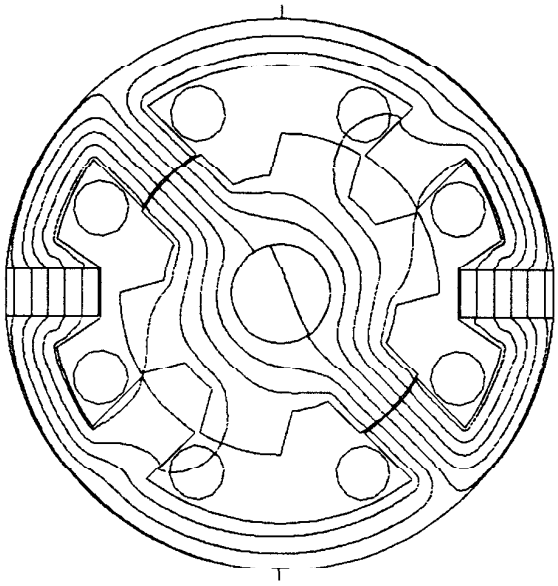

Fig. 7. Flux Distribution of $(DS)^2$PM Motor – Fully Aligned Position without Current

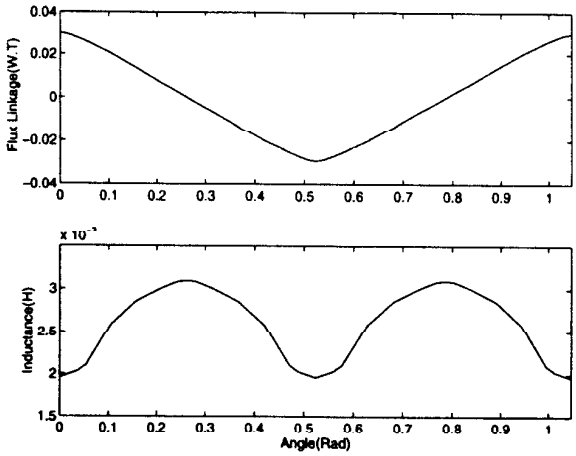

Fig. 8. Flux Linkage and Inductance of a Phase Winding vs. Rotor Position

aligned is shown in Fig. 7. It can be seen that the majority of flux goes through the aligned pole pairs. However, there is portion of the flux passes through the unaligned pole pairs and is not negligible. This leakage flux reduces the power capability of the motor. Its effect will be further discussed in the following section.

In order to determine how flux linkages vary with position, a no load condition is assumed. By rotating the rotor step by step, the flux linkages at different rotor angular positions is obtained by the finite element method. Fig. 8 shows the flux linkage variation vs. the rotor position. The form of the curve is nearly triangular, which corresponds closely to the working principle of the flux-switching. The phase winding inductance is obtained by injecting a small amount of current to the winding. The field solution data is processed to find a flux linkage increment. The winding inductance is obtained by dividing the flux linkage increment by the injected current. The phase winding inductance calculated in this manner is shown in Fig. 8. The flux linkage and inductance of the other phase can be obtained by shifting the curves shown in Fig. 8 by $\frac{\pi}{12}$.

In this calculation, the fully aligned position and half aligned position are of interest, since the flux linkage of phase winding reaches its maximum or minimum at the fully aligned position, while the phase inductance reaches its maximum at half aligned position and its minimum at a fully aligned position. It can be noted that although the flux linkage curve has nearly a triangular form as expected, the curve of inductance variation has a bell shape. The reason for this behavior is that the permeance presented to the winding by rotor movement does not vary linearly as predicted ideally.

IV. Effect of Saturation and Leakage

The assumptions made previously are helpful for the understanding of working principle of $(DS)^2PM$ motor. However, the saturation and fringing effect play an important role in doubly salient PM machines. It is well known that energy exchange between an electromagnetic system and an electric source is given by

$$E = \int id\lambda \tag{10}$$

The locus of flux linkage and current in the flux linkage-current plane as rotor rotates for an electrical cycle is a closed loop. The

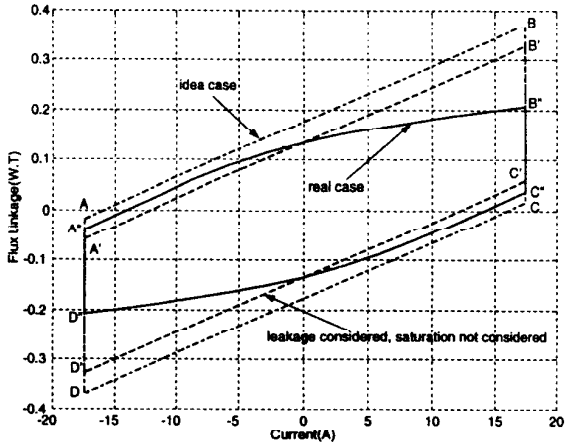

Fig. 9. Flux Linkage vs. Winding Current

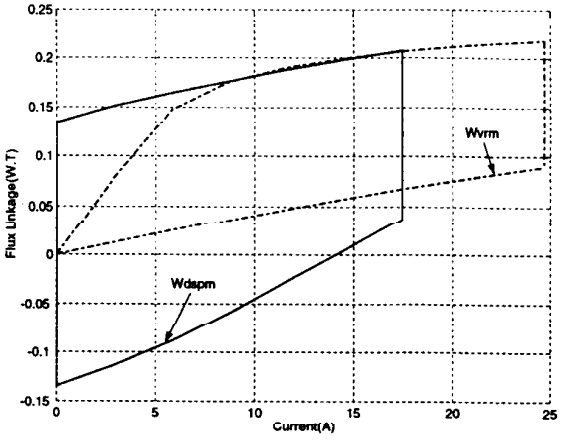

Fig. 10. Comparison between $(DS)^2PM$ and VRM

area enclosed equals the energy converted to mechanical form in one cycle. For $(DS)^2PM$ motor, the current commutation takes place at the position at which one pole pair is fully aligned. For ideal current source, the current reverses instantly. This constraint corresponds to the line AB in Fig. 9 for an ideal motor (i.e., no leakage and saturation). If current is kept constant as the rotor turns for 30°, line BC in Fig. 9 represents the flux linkage vs. current. At this point another pole pair is fully aligned, and current reverses again and the locus moves along line CD. The rotor keeps rotating at constant current, the locus now is line DA as rotor has turned another 30° and complete a cycle. The area enclosed by parallelogram ABCD is the energy converted for 60° rotor rotation.

From Fig. 6, it is clear that the leakage flux going through an unaligned pole pair is not negligible. From the winding connection shown in Fig. 1, it can be seen that the presence of leakage flux reduces the useful flux linkage. This reduction leads to the fact that the winding flux linkage is about 77% of the value for no leakage, the number obtained from FEM analysis. The parallelogram of A'B'C'D' of Fig. 9 represents the energy conversion taking into account of leakage flux, but not the saturation effect.

When saturation of the iron is taken into account, there is a further reduction in the energy conversion. When there is no saturation, the locus of flux linkage vs. current at current commutation is a straight line, assuming commutation completes instantly so that rotor position is not changed. In reality, when current is applied to strengthen the field, the iron saturates and the locus is no longer straight. The enclosed area again becomes smaller and, hence, the converted energy. Note that at zero current the flux linkages of both saturated and non-saturated case are the same. The curve A"B"C"D" enclosed area is the energy converted for the case where both leakage and saturation are taken into account. The FEM analysis results show that saturation effect reduces the amount to about 86% of the unsaturated case. The total reduction due to leakage and saturation is about 1/3, i.e., the real power density is about 2/3 of the ideal case.

It is interesting to compare the $(DS)^2PM$ motor with a conventional variable reluctance machine(VRM) in terms of their torque production capability. Again the VRM has been studied using FEM analysis. For fair comparison, both motors are assumed to have identical main dimension and surface current density, but the air gap length of the VRM is smaller to achieve a saturated design. The flux linkage versus current loci for both machines are obtained from FEM analyses and is shown in Fig. 10. The area W_{vrm} represents the energy conversion in one stroke for VRM, which corresponds to 30° movement. The energy conversion of half cycle for $(DS)^2PM$ machine is represented by area W_{dspm}, which also corresponds to the 30° movement of the rotor. In this case, the torque density of $(DS)^2PM$ machine is 1.36 times of that of the VRM machine, assuming both motors are driven by an ideal current source. In reality, the current waveform of the $(DS)^2PM$ machine is closer to the ideal one than that of the VRM, which means the gain of $(DS)^2PM$ machine would be even more. One factor that works against the $(DS)^2PM$ machine is that the axial length is longer to accommodate the extra end windings and the extra copper associated with it.

V. Coupled Circuit Simulation

The $d-q$ model of an AC machine is well established and widely used in analysis of AC drives. It is based on the assumption that the stator windings and air gap flux density are sinusoidally distributed. However, the assumption is far from reality in some cases, such as the newly emerged doubly salient PM machine [2], and an induction or synchronous reluctance machine under fault conditions (one phase short/open circuit, etc.). A model based on the basic geometry and winding layout of an arbitrary n phase machine would be much more suitable for a general purpose, time domain simulation of an AC machine. In the coupled circuit model of AC machine, the parameters such as mutual inductance and the PM induced flux linkages are considered to be time-varying and can be evaluated in real time, while secondary parameters such as end-turn effect, leakage inductances are treated as constants. The model has been successfully used in the analysis of induction and synchronous reluctance machines[8][9].

A. Simulation Model for General Case

For any electric machine, the circuit equations can be written as

$$V_s = R_s I_s + \frac{d\Lambda_s}{dt} \tag{11}$$

$$V_r = R_r I_r + \frac{d\Lambda_r}{dt} \tag{12}$$

$$\Lambda_s = L_{ss} I_s + L_{sr} I_r + \Lambda_{spm} \tag{13}$$

$$\Lambda_r = L_{rs} I_s + L_{rr} I_r + \Lambda_{rpm} \tag{14}$$

where

R_s — diagonal matrix of stator resistances,
R_r — diagonal matrix of rotor resistances,
L_{ss} — stator inductance matrix,
L_{rr} — rotor inductance matrix,
L_{sr} — stator to rotor mutual inductance matrix,
$L_{rs} = L_{sr}^T$ — rotor to stator mutual inductance matrix,
I_s — stator current vector,
I_r — rotor current vector,
V_s — stator voltage vector,
V_r — rotor voltage vector,
Λ_{spm} — the flux linkage produced solely by magnets and coupled with stator windings,
Λ_{rpm} — the flux linkage produced solely by magnets and coupled with rotor windings.

The power input or output of the machine neglecting the resistive loss is

$$\begin{aligned} p &= I_s^T \frac{d\Lambda_s}{dt} + I_r^T \frac{d\Lambda_r}{dt} \\ &= I_s^T \frac{dL_{ss}}{dt} I_s + I_s^T L_{ss} \frac{dI_s}{dt} + I_s^T \frac{dL_{sr}}{dt} I_r + I_s^T L_{sr} \frac{dI_r}{dt} \\ &\quad + I_s^T \frac{d\Lambda_{pms}}{dt} + I_r^T \frac{dL_{rs}}{dt} I_s + I_r^T L_{rs} \frac{dI_s}{dt} + I_r^T \frac{dL_{rr}}{dt} I_r \\ &\quad + I_r^T L_{rr} \frac{dI_r}{dt} + I_r^T \frac{d\Lambda_{pmr}}{dt} \end{aligned} \tag{15}$$

The stored magnetic field energy of the machine is

$$W_m = \frac{1}{2} I_s^T L_{ss} I_s + I_s^T L_{sr} I_r + \frac{1}{2} I_r^T L_{rr} I_r \tag{16}$$

The derivative of W_m is

$$\begin{aligned} \frac{dW_m}{dt} &= \frac{1}{2} \frac{dI_s^T}{dt} L_{ss} I_s + \frac{1}{2} I_s^T \frac{dL_{ss}}{dt} I_s + \frac{1}{2} I_s^T L_{ss} \frac{dI_s}{dt} \\ &\quad \frac{dI_s^T}{dt} L_{sr} I_r + I_s^T \frac{L_{sr}}{dt} I_r + I_s^T L_{sr} \frac{dI_r}{dt} \\ &\quad \frac{1}{2} \frac{dI_r^T}{dt} L_{rr} I_r + \frac{1}{2} I_r^T \frac{dL_{rr}}{dt} I_r + \frac{1}{2} I_r^T L_{rr} \frac{dI_r}{dt} \end{aligned} \tag{17}$$

The power developed by an electromagnetic system is

$$p = p_{me} + \frac{dW_m}{dt} \tag{18}$$

Notice that

$$\frac{dI_s^T}{dt} L_{ss} I_s = I_s^T L_{ss} \frac{dI_s}{dt}$$

$$\frac{dI_r^T}{dt} L_{rr} I_r = I_r^T L_{rr} \frac{dI_r}{dt}$$

and

$$\frac{dI_s^T}{dt} L_{sr} I_r = I_r^T L_{sr} \frac{dI_s}{dt}$$

Hence, the power converted to mechanical form is

$$\begin{aligned} p_{em} &= p - \frac{dW_m}{dt} \\ &= \frac{1}{2} I_s^T \frac{dL_{ss}}{dt} I_s + I_s^T \frac{dL_{sr}}{dt} I_r + \frac{1}{2} I_r^T \frac{dL_{rr}}{dt} I_r \\ &\quad + I_s^T \frac{d\Lambda_{pms}}{dt} + I_r^T \frac{d\Lambda_{pmr}}{dt} \end{aligned} \tag{19}$$

The corresponding torque produced is

$$\begin{aligned} T_{em} &= \frac{1}{2} I_s^T \frac{dL_{ss}}{d\theta} I_s + I_s^T \frac{dL_{sr}}{d\theta} I_r + \frac{1}{2} I_r^T \frac{dL_{rr}}{d\theta} I_r \\ &\quad + I_s^T \frac{d\Lambda_{pms}}{d\theta} + I_r^T \frac{d\Lambda_{pmr}}{d\theta} \end{aligned} \tag{20}$$

The first term in equation (20) represents the reluctance torque of an AC machine. The fourth term represents the PM torque of the PM machine.

The mechanical equations are

$$\frac{d\omega}{dt} = \frac{1}{J}(T_{em} - T_{load}) \tag{21}$$

$$\frac{d\theta}{dt} = \omega \tag{22}$$

where

θ — the mechanical angle,
ω — mechanical speed,
T_{load} — load torque,
J — the inertia of the rotor and load.

Equations (11), (12), (13), (14), (20), (21) and (22) form the mathematical model for a general electric machine simulation.

B. Simulation Model of $(DS)^2PM$ Motor

For the $(DS)^2PM$ motor, there are no rotor winding resistance, inductance and flux linkage. The voltage equation of the $(DS)^2PM$ motor is

$$V_s = R_s I_s + \frac{d\Lambda_s}{dt} \tag{23}$$

where

$$V_s = \begin{bmatrix} V_a \\ V_b \end{bmatrix} \tag{24}$$

$$R_s = \begin{bmatrix} R_a & 0 \\ 0 & R_b \end{bmatrix} \tag{25}$$

$$I_s = \begin{bmatrix} I_a \\ I_b \end{bmatrix} \tag{26}$$

$$\Lambda_s = \begin{bmatrix} \Lambda_a \\ \Lambda_b \end{bmatrix} \tag{27}$$

The flux linkage equation is

$$\Lambda_s = L_{ss} I_s + \Lambda_{spm} \tag{28}$$

where

$$L_{ss} = \begin{bmatrix} L_{aa} & L_{ab} \\ L_{ba} & L_{bb} \end{bmatrix} \tag{29}$$

$$\Lambda_{spm} = \begin{bmatrix} \Lambda_{spma} \\ \Lambda_{spmb} \end{bmatrix} \tag{30}$$

If the end winding coupling between two phases is neglected, then $L_{ab} = L_{ba} = 0$ is assumed in the simulation.

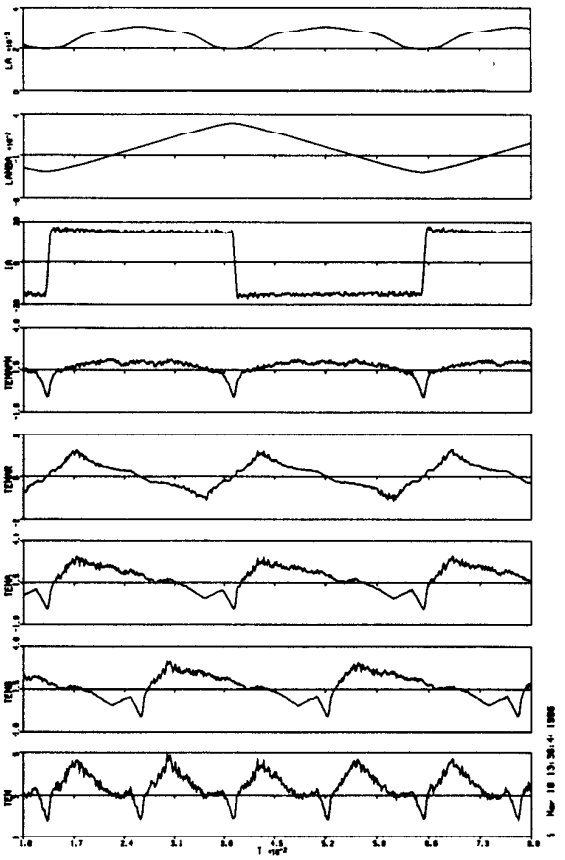

Fig. 11. Simulation – Flux Linkage, Inductance, Current and Torque at Low Speed. Traces from Top Down: 1.phase A inductance, 2.phase flux linkage, 3.phase A current, 4.phase A PM torque, 5.phase A reluctance torque, 6.phase A torque, 7.phase B torque, 8.resultant torque of two phase.

The electromagnetic torque is

$$T_{em} = \frac{1}{2} I_s^T \frac{dL_{ss}}{d\theta} I_s + I_s^T \frac{d\Lambda_{pms}}{d\theta} \tag{31}$$

The mechanical equations are

$$\frac{d\omega}{dt} = \frac{1}{J}(T_{em} - T_{load}) \tag{32}$$

$$\frac{d\theta}{dt} = \omega \tag{33}$$

C. Simulation

A simulation study has been carried out on a prototype $(DS)^2PM$ motor. The flux linkage, phase winding inductance and their derivatives are obtained by linear interpolation of the pre-stored flux linkage and inductance curves. These curves are calculated by processing the FEM analysis data. The converter is composed of two H bridges and a CRPWM control scheme is utilized. Fig. 11 shows the flux linkage, inductance, current, PM torque and reluctance torque of one phase, torque of the two phases and the resultant torque at low speed. It is clear from the plot that the PM torque is always positive, but has

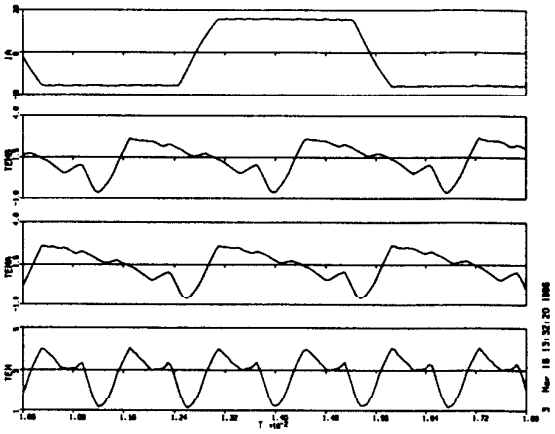

Fig. 12. Simulation – Phase Current and Torque at Medium Speed. Traces from Top down: 1.phase A current, 2.phase B torque, 3.phase A torque, 4.resultant torque.

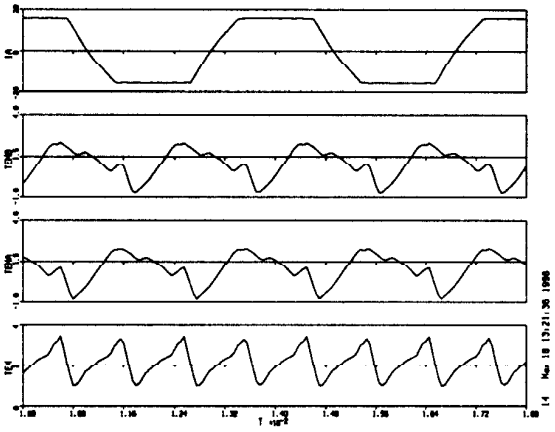

Fig. 13. Simulation – Phase Current and Torque at High Speed. Traces from Top down: 1.phase A current, 2.phase B torque, 3.phase A torque, 4.resultant torque.

notches caused by current commutation, while the reluctance torque pulsates at two times the current fundamental frequency and has zero average value when the current is symmetrical. The resultant torque is always greater than zero so that starting is not a problem. The torque pulsating is less severe and the pulsating frequency of the resultant torque is 4 times that of the current. It can be noted that the reluctance torque cannot be completely canceled due to the bell-shaped inductance variation curve as shown in Fig. 8. It is desirable to reduce the reluctance torque pulsation by decreasing the winding inductance if possible.

The phase current, torque of phase A, B and resultant torque at medium speed are shown in Fig. 12. The current has a trapezoidal form. Fig. 13 shows the traces at high speed. It is shown that at high speed the current commutation delay causes large notches in torque. The advance of commutation triggering may help lessen this problem.

VI. Conclusion

A new dual stator doubly salient permanent magnet motor has been presented in this paper and its working principle has been demonstrated. The main advantages of $(DS)^2PM$ motor are:

- high torque density due to the 180° conducting trapezoidal current interval compared to 120° for a 6 pole 3 phase $DSPM$ or VRM.
- high efficiency due to the use of PM material.
- simple and rugged rotor structure, good high speed capability.
- greatly reduced torque ripple.

However, as shown by the FEM analysis and the dynamic simulation, this type of machine still has torque pulsation. This is inherent property of all doubly salient machines due to the nonlinear variation of reluctance. The major disadvantages are:

- longer axial size and extra copper use due to the extra end winding.
- relatively high leakage flux.

Considering the gain in power density and efficiency, it is concluded that the $(DS)^2PM$ drive has potential to compete with conventional AC drives in smaller frame sizes.

VII. Acknowledgment

The authors thank EPRI for their support of this research project.

References

[1] S.E. Rauch and L.J. Johnson, *Design Principles of Flux-Switch Alternators*, AEEE Trans. Dec. 1955, pp. 1261-1268

[2] Y. Liao, *Design and Performance Evaluation of a New Class of Permanent Magnet Motors with Doubly Salient Structure*, Ph.D. Thesis, University of Wisconsin-Madison, September 1992

[3] Y. Liao, F. Liang and T. A. Lipo, *A Novel Permanent Magnet Motor with Doubly Salient Structure*, IEEE Transactions on Industry Applications, Vol. IA-31, No. 5, Sept/Oct 1995, pp. 1069-1078

[4] A. Shakal, Y. Liao and T.A. Lipo, *A New Permanent Magnet Motor with True Field Weakening*, IEEE International Symposium on Industrial Electronics, Budapest, Hungary, June 1993, pp. 19-24

[5] B. Sarlioglu, Y. Zhao and T.A. Lipo, *A Novel Doubly Salient Single Phase Permanent Magnet Generator*, IEEE IAS annual Meeting, Oct. 1993, pp. 9-15

[6] Y. Li, *Design and Control of a New Class of Doubly Salient Permanent Magnet Machines*, Ph.D. Thesis, University of Wisconsin-Madison, December 1995

[7] Y. Li, F. Leonardi and T.A. Lipo, *A Novel Doubly Salient Permanent Magnet Generator Capable of Field Weakening*, Conference on Design to Manufacture in Modern Industry(DMMI), Lake bled, Slovenia, May 19-30, 1995

[8] X. Luo, Y. Liao, H. Toliyat, A. El-Antably and T. A. Lipo, *Multiple Coupled Circuit Modeling of Induction Machines*, IEEE Transactions on Industry Applications, Vol. IA-31, No. 2, March/April 1995, pp. 311-318

[9] X. Luo, A. El-Antably and T. A. Lipo, *Multiple Coupled Circuit Modeling of Synchronous Reluctance Machines*, IEEE Industry Applications Soc. Conf. Rec., Vol. 1, pp.281-289, 1994